Analysis of the Role of the KMSKS Loop in the Catalytic Mechanism of the Tyrosyl-tRNA Synthetase Using Multimutant Cycles

Eric A. First‡ and Alan R. Fersht*

MRC Unit for Protein Function and Design, Cambridge Centre for Protein Engineering, University Chemical Laboratory, Lensfield Road, Cambridge CB2 1EW, U.K.

Received October 28, 1994; Revised Manuscript Received February 2, 1995⊗

ABSTRACT: A mobile loop in tyrosyl-tRNA synthetase, which corresponds to the KMSKS signature sequence of class I aminoacyl-tRNA synthetases, destabilizes the E·Tyr·ATP complex but stabilizes the following E·[Tyr-ATP]‡ transition state for the formation of E·Tyr-AMP. Three amino acid residues in the mobile loop, K230, K233, and T234, are known to be primarily responsible for these effects. We now analyze the network of interactions between these three amino acids using multiple mutant free energy cycles. The complete characterization of the coupling energies within the mobile loop allows each of the steps leading to the formation of the transition state complex to be dissected into its energetic components. In particular, it is found that, in the absence of a functional mobile loop, there is synergistic coupling between the tyrosine and ATP substrates (i.e., each enhances the binding affinity of the other) which stabilizes the E·Tyr·ATP intermediate preceding the transition state complex. Thus, the mobile loop disrupts the synergism between the ATP and tyrosine substrates, using the ATP binding energy to stabilize the transition state for the reaction. Whereas the net effect of the mobile loop in the E·Tyr·ATP complex results from several conflicting side chain interactions that tend to offset each other, conflicting interactions in the E·[Tyr-ATP]‡ transition state complex have been minimized and stabilizing pairwise interactions between the K230, K233, and T234 side chains are optimized. The tight coupling between the side chains of K230, K233, and T234 suggests that the mobile loop adopts a highly constrained conformation during formation of the transition state complex. These results quantitatively demonstrate the importance of side chain interactions in enzyme catalysis and illustrate the use of binding energy to stabilize the transition state of a reaction and the presence of unfavorable interactions to destabilize the ground state.

The understanding of the molecular basis of enzyme catalysis can be divided into two parts: elucidating the structural basis by which catalysis is achieved; and elucidating the energetic basis of catalysis. While X-ray crystallography and NMR spectroscopy can establish a structural basis, understanding the energetics of the reaction is the domain of kinetic and thermodynamic analyses. For enzyme-catalyzed reactions in general (and demonstrated directly for the tyrosyl-tRNA synthetase in particular) both specificity and rate enhancement are achieved through the use of the binding energy between the enzyme and its substrate(s) (Fersht, 1987). Thus, to understand how an enzyme such as tyrosyl-tRNA synthetase catalyzes a particular reaction, one must analyze the energetics of the interaction between the enzyme and its substrate(s) for each step along the reaction pathway. Site-directed mutagenesis has proven invaluable in these analyses, as it allows the interactions between the substrate(s) and specific amino acid side chains to be evaluated. To understand fully the catalytic mechanism of an enzyme, however, it is necessary to analyze not only the energetics of the interaction between an amino acid side chain and the substrate(s) but also the effect that interactions between amino acid side chains have on the energetics of the reaction. In enzyme catalysis, it is possible that several amino acids may be energetically coupled in a manner that affects either the rate or specificity of catalysis. Thermodynamic free energy cycles provide a method by which the effect that these couplings have on catalysis can be evaluated (Carter et al., 1984; Horovitz, 1987; Horovitz & Fersht, 1990, 1992; Fersht et al., 1992).

Aminoacyl-tRNA synthetases catalyze the charging of tRNA by amino acids in a two-step reaction involving: (1) the activation of the amino acid by ATP, and (2) the charging of tRNA by this activated amino acid. The aminoacyl-tRNA synthetases can be divided into two distinct classes on the basis of their "signature" sequences. Class I aminoacyl-tRNA synthetases (corresponding to glutamine, tyrosine, methionine, glutamic acid, arginine, valine, isoleucine, leucine, tryptophan, and cysteine) all contain two signature sequences: H-X-G-H and K-M-S(T)-K-S(T) (Webster et al., 1984; Hountondji et al., 1986). X-ray crystallographic analysis of the tyrosyl-, methionyl-, and glutaminyl-tRNA synthetases indicates that the tertiary structure of the ATP-binding domain is similar in this class of enzymes (Bhat et al., 1982; Brunie et al., 1990; Rould et al., 1991). In contrast, the class II aminoacyl-tRNA synthetases, which possess a conserved proline and the signature sequences F-R-X-E and G-X-G-X-G-X-E-R (Eriani et al., 1990), adopt a tertiary structure which is distinct from that found in the class I aminoacyl-tRNA synthetases (Cusack et al., 1990). Class I aminoacyl-tRNA synthetases aminoacylate the 2′-hydroxyl group of the terminal ribose, whereas class II aminoacyl-tRNA synthetases aminoacylate the 3′-hydroxyl group (Moras, 1992).

‡ E.A.F. is a recipient of NIH postdoctoral fellowship 1 F32 GM12023-01. Current address: Department of Biochemistry, School of Medicine in Shreveport, Louisiana State University Medical Center, 1501 Kings Highway, P.O. Box 33932, Shreveport, LA 71130-3932.

⊗ Abstract published in *Advance ACS Abstracts,* April 1, 1995.

0006-2960/95/0434-5030$09.00/0

The KMSKS signature sequence of the class I aminoacyl-tRNA synthetases is homologous to the "Walker" sequence found in a number of other nucleotide-binding enzymes (Walker et al., 1982, 1984). In addition, the tertiary structure displays a "Rossman fold" which is characteristic of nucleotide-binding enzymes (Rossman et al., 1974). In tyrosyl-tRNA synthetase, Fersht et al. (1988) have shown that a key component of catalysis in the first step of the reaction is stabilization of the enzyme-bound tyrosyl adenylate by a "mobile" loop containing the KMSKS signature sequence. The actual signature sequence in tyrosyl-tRNA synthetase is K^{230}-F-G-K-T^{234}. Three amino acids, lysine 230 (K230), lysine 233 (K233), and threonine 234 (T234), substantially stabilize the transition state complex (Fersht et al., 1988; First & Fersht, 1993a). Moreover, deletion of the entire "mobile" loop shows that it is involved both in destabilizing the E·Tyr·ATP complex preceding the transition state and in stabilizing the E·[Tyr-ATP]‡ transition state complex. Both analysis of a loop deletion mutant (First & Fersht, 1993c) and preliminary analyses of a *K230A/T234A* double mutant (First & Fersht, 1993a) suggest that couplings between the amino acid residues in this mobile loop are crucial to its role in catalyzing the formation of tyrosyl adenylate.

In this paper, the effect that couplings between amino acid side chains within the mobile loop of tyrosyl-tRNA synthetase from *Bacillus stearothermophilus* have on catalysis are analyzed. For this purpose, double and triple alanine mutants involving K230, K233, and T234 have been constructed. These mutants, together with the single alanine mutants at these positions (Fersht et al., 1988; First & Fersht 1993a,b) constitute a "triple mutant cube" which allows the energetics of the couplings between K230, K233, and T234 to be analyzed for each step in the reaction pathway up to, and including, the formation of the E·[Tyr-ATP]‡ transition state complex. The results of these investigations provide a detailed picture of the energetic basis for the involvement of the mobile loop in the catalysis of tyrosyl adenylate formation by tyrosyl-tRNA synthetase.

THEORY

Kinetic analysis of single mutants is frequently used to identify specific interactions between an enzyme and its substrate(s). Analysis of this type of experiment is complicated by the possibility that mutation of the amino acid not only affects the specific side chain−substrate interaction of interest but also disrupts interactions with amino acid side chains surrounding the mutation. The functional importance of these side chain−side chain couplings in stabilizing a particular reaction step can be quantified using double mutant free energy cycles (Carter et al., 1984; Horovitz, 1987). Consider the double mutant cycle shown in Figure 1 involving two wild-type amino acid side chains, i and j. In this double mutant cycle, the deletion of a wild-type amino acid side chain (i.e., a mutation to alanine) is denoted by "0", and the reference protein is defined to be the double alanine mutant (0,0 in Figure 1). The free energy change for the 0,0 → i,0 transition, ΔG_a, corresponds to the introduction of side chain i in the absence of side chain j (i.e., ΔG_a contains no i,j coupling terms). In contrast, the free energy change associated with the 0,j → i,j transition (ΔG_d) contains two terms: one term corresponding to the introduction of side chain i in the absence of side chain j

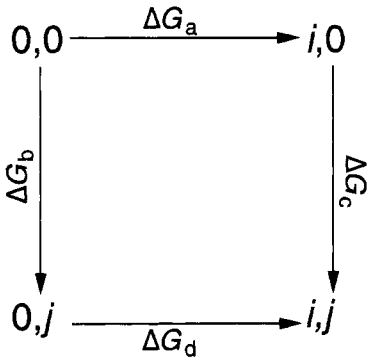

FIGURE 1: Hypothetical double mutant cycle. A hypothetical double mutant cycle involving the replacement of two alanine side chains (indicated by "0") by the amino acid side chains i and j. ΔG_a, ΔG_b, ΔG_c, and ΔG_d are the changes in apparent free energies of binding ($-\Delta^2 G_{app}$) for the conversion of each alanine to side chains i and j. In keeping with the nomenclature introduced in eqs 1−4, a single delta is used for these transitions, although technically there should be two deltas since the free energies for binding to each enzyme−substrate complex are measured relative to the free energy for the free enzyme (which has been defined to be zero).

(ΔG_a) and one term corresponding to the coupling between side chains i and j ($\Delta^2 G_{int}$). The coupling energy, $\Delta^2 G_{int}$, is calculated from the difference between ΔG_a and ΔG_d. (Alternatively, $\Delta^2 G_{int}$ can be calculated from the difference between ΔG_b and ΔG_c as the additivity of the free energy cycle requires that $\Delta G_d - \Delta G_a = \Delta G_c - \Delta G_b$.) If the energetic effects of the mutations are independent of each other, then $\Delta G_d = \Delta G_a$ (and $\Delta G_c - \Delta G_b$) so that $\Delta^2 G_{int} = 0$, and the changes of energy on mutation are said to be nonadditive. The coupling energy is the quantitative measure of the magnitude of how the effects of mutations are coupled or differ from nonadditivity. It is not known, and it is not assumed in this analysis, whether the coupling results from direct interactions between the residues concerned or it is mediated via other groups in the protein (or by the solvent).

The above analysis can be extended to higher order couplings involving more than two different side chains. For example, the triple mutant cube shown in Figure 2 can be separated into six different double mutant cycles (each face of the cube corresponding to one cycle). By comparing the $\Delta^2 G_{int}$ values for cycles located on opposing faces of the triple mutant cube, one obtains the free energy of coupling that corresponds to the effect that a third amino acid has on the coupling between two other amino acids (e.g., $\Delta^3 G_{int} = \Delta^2 G_{int}^{T234} - \Delta^2 G_{int}^{T234A}$, where $\Delta^2 G_{int}^{T234}$ and $\Delta^2 G_{int}^{T234A}$ correspond to the cycles in Figure 1 in which all mutants contain T234 and *T234A*, respectively). Owing to the additivity of energetics within the cube, the $\Delta^3 G_{int}$ values calculated from any of the three pairs of opposing faces of the cube will be equivalent.

In general, the coupling between n different amino acid side chains can be calculated by the following equation (Horovitz & Fersht, 1992):

$$\Delta^n G_{int} = \sum_{r=1}^{n} (-1)^{r+n} \sum_{\alpha=1}^{(n_r)} \Delta G_{r,\alpha} \qquad (1)$$

where n is the total number of side chains being added, r is the number of additions in a given molecule ($r \leq n$), (n_r) are the binomial coefficients, and α represents the different possible combinations for each r value. For pairwise and

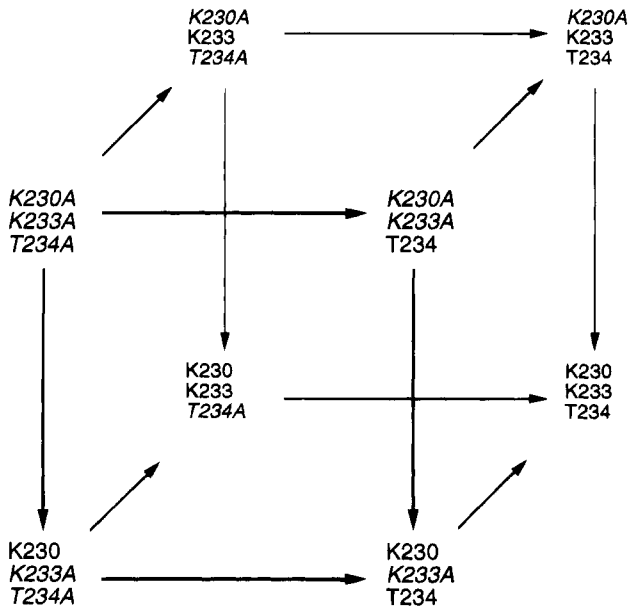

FIGURE 2: Interrelationships between the wild-type enzyme and mobile loop mutants. A triple mutant cube is shown which indicates the interrelationships between the wild-type enzyme and mobile loop mutants at positions K230, K233, and T234. The starting point for this cube is the *K230A/K233A/T234A* triple alanine mutant (italics denote mutations). Arrows point from the more highly mutated species to the less highly mutated species. Opposing faces of the cube represent identical double mutant cycles except that the identity of the amino acid side chain at the third position is altered. The triple mutant cube is shown as isolated double mutant cycles in Figures 4, 5, and 6.

ternary couplings this equation simplifies to (Horovitz & Fersht, 1992)

$$\Delta^2 G_{\text{int}} = \Delta G_2 - \sum \Delta G_1 \quad (2)$$

$$\Delta^3 G_{\text{int}} = \Delta G_3 - \sum \Delta G_2 + \sum \Delta G_1 \quad (3)$$

where ΔG_1 is the free energy change for the addition of each individual side chain in the absence of the other two side chains (i.e., ΔG_i, ΔG_j, and ΔG_k), ΔG_2 is the free energy change for the simultaneous addition of any two side chains in the absence of the third side chain (i.e., $\Delta G_{i,j}$, $\Delta G_{i,k}$, and $\Delta G_{j,k}$), and ΔG_3 is the free energy change for adding all three side chains, i, j, and k, simultaneously (i.e., $\Delta G_{i,j,k}$).

Interpretation of the effect that coupling between n different amino acid side chains has on the stability of a particular enzyme−substrate complex is facilitated by eq 4 (Horovitz & Fersht, 1992):

$$G_n = G_o + \sum \Delta G_1 + \sum \Delta^2 G_{\text{int}} + \sum \Delta^3 G_{\text{int}} + \ldots + \Delta^n G_{\text{int}} \quad (4)$$

where G_o is the energy of the reference protein, G_n is the energy when n side chains have been added, $\sum \Delta G_1$ is as defined above, and $\sum \Delta^2 G_{\text{int}}$, $\sum \Delta^3 G_{\text{int}}$, ..., $\Delta^n G_{\text{int}}$ are the sums of the coupling terms for the 2, 3, ..., n dimensions. Specifically, one can compare the G_n value determined experimentally, $G_{n(\text{expt})}$, with the G_n value that is calculated if there is no coupling in the nth dimension (i.e., $\Delta^n G_{\text{int}} = 0$), $G_{n(\text{add})}$. Although the absolute values for G_o, $G_{n(\text{expt})}$, and $G_{n(\text{add})}$ are inaccessible, their relative values can be determined for various enzyme−substrate complexes if the free enzyme is defined as the reference state (i.e., $G_E = 0$). For the E·Tyr·ATP complex in tyrosyl-tRNA synthetase, for example, $G_{\text{E·Tyr·ATP}}$ for the most highly mutated enzyme species in each cycle is designated G_o, the free energy for the reference protein in the E·Tyr·ATP complex relative to its free energy in the free enzyme state (Wells & Fersht, 1986). Similarly, $G_{\text{E·Tyr·ATP}}$ for the least mutated enzyme species in each cycle is designated as $G_{n(\text{expt})}$.

EXPERIMENTAL PROCEDURES

Materials. All enzymes were obtained from United States Biochemicals, chemicals from Sigma Chemicals (London) and radiochemicals from Amersham International.

Production of Mutants. All mutants were constructed using the method of Kunkel (1985) from pYTS5, a pTZ18u phagemid which contains the wild-type tyrosyl-tRNA synthetase gene from *B. stearothermophilus* preceded by a Trp-Lac promoter. Construction of this phagemid vector is described elsewhere (First & Fersht, 1993a). The oligonucleotides used in the mutagenesis were as follows (mismatches are shown in italics): 5′ CT TTC CGT T*GC* CCC GAA T*GC* CGT GCC GTC 3′ (*K230A/K233A*/T234), 5′ GCG GCT TTC CG*C* TTT CCC GAA T*GC* CGT GCC GTC CG 3′ (*K230A*/K233/*T234A*), 5′ CG GCT TTC CG*C* T*GC* CCC GAA TTT 3′ (K230/*K233A/T234A*), and 5′ GCG GCT TTC CG*C* T*GC* CCC GAA T*GC* CGT GCC GTC CG 3′ (*K230A/K233A/T234A*). Uracil-containing pYTS5 template was purified from *Escherichia coli* CJ236. Mutagenesis reactions were transformed into *E. coli* TG2 cells [*rec*A form of TG1 (Gibson, 1984)], and mutants were screened by dideoxy sequencing of the phagemid templates. Single-stranded template was isolated from positive clones and retransformed into *E. coli* TG2 cells, and single-stranded template was repurified from these cells. The entire tyrosyl-tRNA synthetase gene for each mutant was sequenced to ensure no other mutations were present. All transformations were done using the method of Hanahan (1985).

Purification of Enzymes. Mutant enzymes were expressed in *E. coli* TG2 host cells and purified to electrophoretic homogeneity as described previously (First & Fersht, 1993a).

Kinetic Procedures. All experiments were performed at 25 °C in a standard buffer containing 144 mM Tris-HCl (pH 7.78) and 10 mM $MgCl_2$. ATP was added as the magnesium salt to maintain the free Mg^{2+} at 10 mM. The final pH values of the reaction solutions were checked and found to be 7.8.

Activation. The kinetics was analyzed according to Scheme 1. The rate constants for the formation of enzyme-bound tyrosyl adenylate by all mutants were followed by nitrocellulose filter assays (Calendar & Berg, 1966; Leatherbarrow & Fersht, 1987) as described by First and Fersht (1993a). The kinetic constants k_3 (the rate constant for E·Tyr·ATP → E·Tyr-AMP·PP_i) and K_{ATP} (the dissociation constant of E·ATP) were calculated from the variation of k_{obs} with ATP concentration. The dissociation constants for ATP in the absence of bound tyrosine, designated K'_{ATP}, were determined according to the procedure described by Wells et al. (1991). The assays used are essentially identical to those described for the determination of K'_{ATP} values except: (1) 0.5 μM [^{14}C]tyrosine was used instead of 50 μM [^{14}C]tyrosine, and (2) ATP concentrations between 0.2 and 10 mM were used. The error in the measurement of dissociation constants was calculated as the standard deviation from the mean of 3−5 different repetitions.

Scheme 1

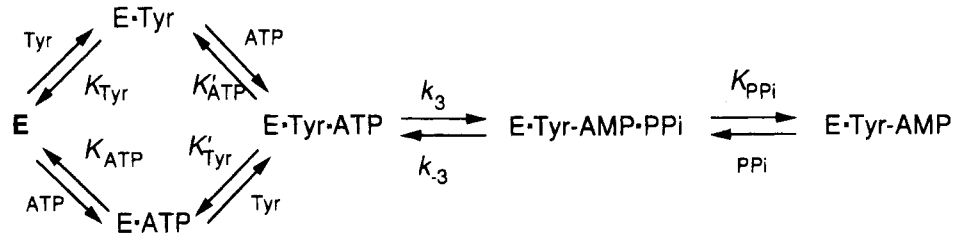

Binding of Tyrosine. The K_{Tyr} (dissociation constant of E·Tyr) for all mutants was determined by equilibrium dialysis as described previously (Fersht, 1975).

Pyrophosphorolysis. Enzyme-bound tyrosyl adenylates were prepared and stored as described by Fersht et al. (1988). Pyrophosphorolysis was initiated by the addition of tetrasodium pyrophosphate to a solution of 100−400 nM E·[^{14}C]-Tyr-AMP in 144 mM Tris-HCl (pH 7.78) and 10 mM $MgCl_2$. Both solutions were preincubated at 25 °C prior to the start of the reaction.

Analysis of Kinetics. Kinetic analysis has been previously described (Fersht et al., 1988; Wells et al., 1991).

Calculation of Interaction Energies. The energy levels for each step in the reaction are calculated relative to the energy level of free enzyme (i.e., $G_E = 0$) for each mutant as described by Wells and Fersht (1986). The apparent binding energy, $-\Delta^2G_{app}$, is calculated by subtracting the free energy change for formation of the relevant complex of the wild-type enzyme from that of the mutant enzyme (Wells & Fersht, 1986). For the E·Tyr complex, for example, $-\Delta^2G_{app} = -[\Delta G_{E\cdot Tyr}(mutant) - \Delta G_{E\cdot Tyr}(wild\text{-}type)]$, where $\Delta G_{E\cdot Tyr}$(wild-type) is the free energy of formation of the E·Tyr complex from E and Tyr as calculated by Wells and Fersht (1986). For double mutant cycles, the $-\Delta^2G_{app}$ associated with each step in the cycle is calculated as the difference between the energy levels for the two enzyme species in the step of the cycle.

Pairwise, ternary, and quaternary coupling energies are calculated as described by Horovitz and Fersht (1992). For pairwise couplings, Δ^2G_{int}, the coupling energy between two side chains, designated *i* and *j*, is calculated from eq 2. In all cases, the reference protein is the protein species in the double mutant cycle which contains the greatest number of amino acids that have been mutated to alanine (e.g., for the double mutant cycle in which *K230A/K233A*/T234 is converted to K230/K233/T234, the *K230A/K233A*/T234 double alanine mutant is the reference protein). For ternary couplings, Δ^3G_{int}, the effect of a third amino acid side chain, *k*, on the pairwise coupling between two other amino acid side chains, *i* and *j*, is calculated from eq 3. The reference protein for these calculations is the *K230A/K233A/T234A* triple mutant. For pairwise, ternary, and quaternary couplings involving the tyrosine substrate as the fourth variable, the reference protein is *K230A/K233A/T234A*, with the tyrosine substrate present at 0.5 μM concentration. Δ^4G_{int}, the effect that any one of the four variables has on the coupling between the other three variables, is calculated from eq 1, where $n = 4$. Errors in the free energy calculations were calculated as the square root of the sum of the squares for the errors in each component of the calculation.

As the K_{ATP} and K'_{ATP} values for the K230/*K233A*/T234 mutant were determined in the presence of 0.5 M NaCl (First & Fersht, 1993b), the free energy values for the E·ATP, E·Tyr·ATP, and E·[Tyr-ATP]‡ complexes of this mutant were calculated using K_{ATP} and K'_{ATP} values for the K233 mutant that were determined in the presence of 0.5 M NaCl, then normalized to conditions in which no NaCl was present using the K_{ATP} and K'_{ATP} values of wild-type enzyme determined both in the presence of 0.5 M NaCl and in the absence of NaCl as reference states. While it is conceivable that this may affect the values calculated for the coupling constants, it is unlikely that such effects are significant for the following reasons: (1) only the K_{ATP} and K'_{ATP} values were determined in the presence of 0.5 M NaCl, all other values being determined under the standard assay conditions; (2) the effect of 0.5 M NaCl on the wild-type enzyme alters the K_{ATP} and K'_{ATP} values by less than 2-fold, changing the $-\Delta G_{app}$ values by 0.3 kcal/mol, a value similar to the experimental error calculated for the free energies of coupling; (3) increased NaCl presumably alters the K_{ATP} and K'_{ATP} values through effects on a number of amino acid residues which, with the exception of K233, are common to both the wild-type enzyme and the K230/*K233A*/T234 mutant, so since free energies of coupling are calculated from the difference between $-\Delta G_{app}$ values for these two enzymes, most of the effects will cancel each other out in the free energy of coupling calculations; (4) as the primary effect of adding NaCl is to disrupt long range ionic interactions, it is unlikely that it has much effect on the observed coupling which (due to the proximity of K230, K233, and T234 in the primary structure) presumably involves mainly short-range interactions; and (5) the free energies of coupling present a consistent picture, regardless of whether the K230/*K233A*/T234 mutant is in the particular cycle from which the Δ^2G_{int} is calculated, this being especially evident in the E·[Tyr-ATP]‡ complex.

RESULTS

Evidence that K230, K233, and T234 Interact in the Wild-Type Enzyme. It has previously been shown that three amino acids, K230, K233, and T234, are responsible for nearly all of the catalytic effects of the mobile loop in tyrosyl-tRNA synthetase (First & Fersht, 1993c). As shown in Figure 3, the effect that mutation of any of these amino acids has on the stability of the intermediate complexes preceding and including the E·[Tyr-ATP]‡ complex is highly dependent on the identity of the other two amino acids. This is indicative of the existence of coupling between these three amino acid side chains in the wild-type enzyme. Analysis of the Δ^2G_{int} values confirms the existence of coupling between the three wild-type amino acids for the E·ATP, E·Tyr·ATP, and E·[Tyr-ATP]‡ complexes (Figure 4). In addition, comparison of Δ^2G_{int} values determined when the third amino acid is the wild-type residue [e.g., K230:K233 (T234) in Figure 4] with Δ^2G_{int} values determined when the third amino acid is

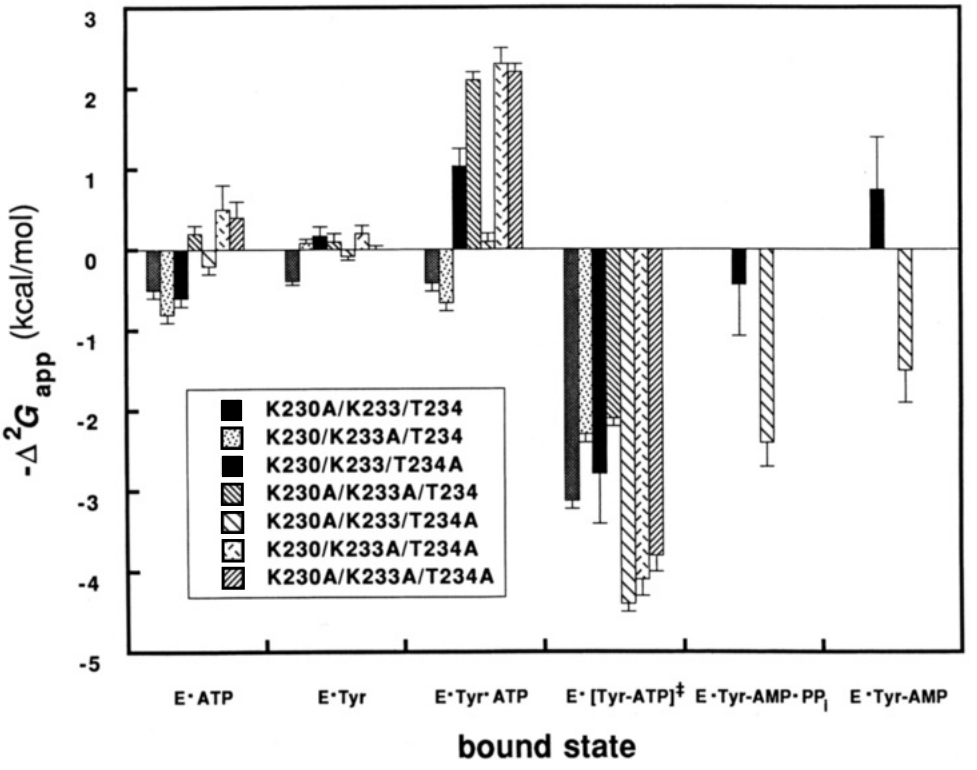

FIGURE 3: Δ^2G_{app} for mobile loop mutants. Tyrosyl-tRNA synthetase is represented by E, "·" represents noncovalent association, and "–" represents covalent bonds between species. The transition state is indicated by "‡". The differences in free energies between the complexes of the mutant and wild-type enzymes are shown for each step leading to the formation of the tyrosyl adenylate intermediate. The energies are in terms of $-\Delta^2G_{app}$, the negative sign is used to be consistent with other notations. Negative values of $-\Delta^2G_{app}$ for a particular complex indicate that the wild-type side chain stabilizes the complex relative to the alanine mutant (e.g., for all the interactions in the E·[Tyr-AMP]‡ complex). Values for *K230A*, *K233A*, and *T234A* are taken from Fersht et al. (1988) and First and Fersht (1993a,b). Errors (bars) are calculated as $e_t = (\sum\chi_i^2)^{1/2}$, where e_t is the total error in $-\Delta^2G_{app}$, and χ_i is the error for each rate or binding constant used to calculate the free energies of binding.

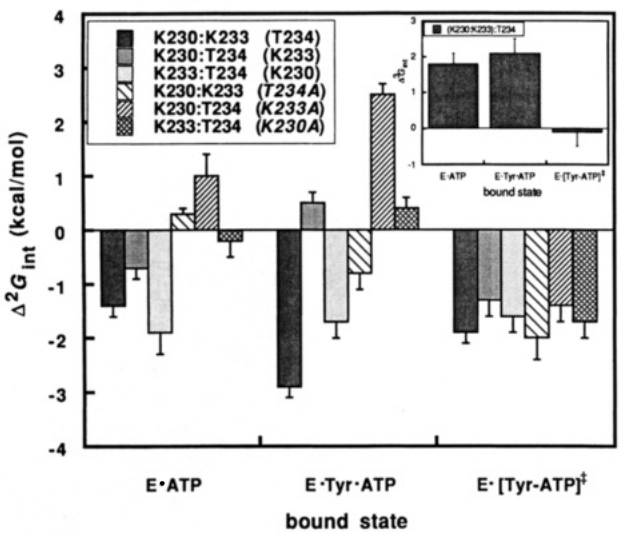

FIGURE 4: Pairwise and ternary coupling values for the E·ATP, E·Tyr·ATP, and E·[Tyr-ATP]‡ complexes. The effects of pairwise coupling on the stabilities of the E·ATP, E·Tyr·ATP, and E·[Tyr-ATP]‡ complexes are shown for each of the side chain pairs. The identity of the third (invariant) amino acid side chain is indicated in parentheses. The effect that ternary coupling between the K230, K233, and T234 side chains has on the stability of the E·ATP, E·Tyr·ATP, and E·[Tyr-ATP]‡ complexes is shown as an inset. Negative Δ^2G_{int} and Δ^3G_{int} values for a particular complex indicate that the coupling between wild-type amino acid side chains that corresponds to the Δ^2G_{int} or Δ^3G_{int} value stabilizes the complex. Errors (bars) are calculated as described in the legend to Figure 3.

alanine [e.g., K230:K233 (*T234A*) in Figure 4] indicate that ternary coupling exists between the three wild-type side chains in the E·ATP and E·Tyr·ATP complexes, but not in the E·[Tyr-ATP]‡ transition state complex. Quantitative analysis of the Δ^3G_{int} term confirms this to be the case (Figure 4, inset). The precise effects of the ΔG_1, Δ^2G_{int}, and Δ^3G_{int} terms are discussed below in relation to the net effect that the mobile loop has on catalysis.

It should be noted that the frame of reference used in Figures 4–7 is opposite to that used previously (i.e., Carter et al., 1984; Fersht & Fersht, 1993b). In other words, in previous papers, the starting point (reference protein) for the double mutant cycles was the wild-type protein, while in this paper, the starting point is the double or triple alanine mutant. This has been done for two reasons: (1) to be consistent with the theory presented earlier in the paper, and (2) to facilitate interpretation of the effect that the higher order couplings have on the stabilities of the enzyme–substrate complexes (i.e., negative values for Δ^2G_{int} and Δ^3G_{int} terms indicate that, in the wild-type enzyme, the coupling stabilizes the enzyme–substrate complex). It should also be noted that instead of plotting Δ^2G_{app} values for each bound state, as is normally done (e.g., First & Fersht, 1993c), $-\Delta^2G_{app}$ values are plotted in Figure 3 in order to be consistent with the frame of reference used in Figures 4–7 (e.g., a negative value for $-\Delta^2G_{app}$ indicates that addition of the wild-type side chain stabilizes the protein).

Contribution of the Mobile Loop to the Stability of the E·Tyr Complex. As indicated in Table 1, none of the mobile loop mutants investigated substantially alters the affinity of the enzyme for the tyrosine substrate. This is consistent with the results of previous investigations (Fersht et al., 1988;

Table 1: Kinetic Constants for the Formation of E·Tyr-AMP by Tyrosyl-tRNA Synthetase and Its Mutants[a]

enzyme	K_{Tyr} (μM)	K_{ATP} (mM)	K'_{ATP} (mM)	k_3 (s^{-1})	k_3/K'_{ATP} (s^{-1} M^{-1})	k_{-3} (s^{-1})	K_{PPi} (mM)	k_{-3}/K_{PP} (s^{-1} M^{-1})
K230/K233/T234[b,c]	12	3.5	4.7	38	8080	16.6	0.61	27 200
K230A/K233/T234[b]	23	8 ± 1	4.9	0.39	80			130
K230/*K233A*/T234[d]	10.4	14 ± 2 [7 ± 0.8]	13 ± 2 [22 ± 2]	0.55	40			
K230/K233/*T234A*	10 ± 1	9 ± 1	1.1 ± 0.4	$7.0 \times 10^{-2} \pm 1 \times 10^{-2}$	60	0.31 ± 0.03	4.4 ± 0.8	70
K230A/*K233A*/T234	12 ± 2	2.5 ± 0.1	0.16 ± 0.04	$1.0 \times 10^{-3} \pm 2 \times 10^{-4}$	0.33			
K230A/K233/*T234A*	14 ± 2	5.1 ± 0.8	3.0 ± 0.3	$1.1 \times 10^{-2} \pm 2 \times 10^{-3}$	3.7	0.37 ± 0.03	2.8 ± 0.5	0.13
K230/*K233A*/*T234A*	10 ± 2	1.7 ± 0.9	0.14 ± 0.03	$8 \times 10^{-4} \pm 2 \times 10^{-4}$	5.7			
K230A/*K233A*/*T234A*	15 ± 2	2.1 ± 0.5	0.1 ● 0.02	$1.2 \times 10^{-3} \pm 5 \times 10^{-4}$	12			

[a] K_{Tyr} is the dissociation constant of the E·Tyr complex, K_{ATP} that of the E·ATP complex, K'_{ATP} the dissociation constant of ATP from the E·Tyr·ATP complex, K_{PPi} the dissociation constant of PP_i from the E·Tyr-AMP·PP_i complex, k_3 is the rate constant for E·Tyr·ATP → E·Tyr-AMP·PP_i, and k_{-3} is the rate constant for the reverse reaction. Standard errors are indicated after each kinetic constant. [b] All values except those for K_{ATP} are taken from Fersht et al. (1988). [c] The K_{ATP} value is taken from Wells et al. (1991). [d] K_{Tyr} value taken from Fersht et al. (1988). K_{ATP} and K'_{ATP} values cannot be accurately determined in the absence of 0.5 M NaCl (First & Fersht, 1993b) and have been corrected for the effect of 0.5 M NaCl. The K_{ATP} value shown was calculated from the K_{ATP} obtained in the presence of 0.5 M NaCl (shown in square brackets beside the corrected K_{ATP} value) using the equality K_{ATP}(*K233A*, 0.0 M NaCl)/K_{ATP}(*K233A*, 0.5 M NaCl) = K_{ATP}(wild type, 0 mM NaCl)/K_{ATP}(wild type, 0 mM NaCl). The corrected K'_{ATP} value was calculated in an analogous manner.

Table 2: The Net Contribution of Each Free Energy Term on the Catalytic Effects of the Mobile Loop (Residues K230, K233, and T234)[a]

complex	G (complex − free)$_{wt}$	G_o (complex − free)$_{mut}$	$\sum\Delta G_1$ (sum of energies of all single mutations)	$\sum\Delta^2 G_{int}$ (sum of all pairwise coupling energies)	$\Delta^3 G_{int}$
E·ATP[b]	−3.35	−3.66	0.5	1.9	−2.1
E·Tyr·ATP[c]	−9.90	−12.05	2.2	2.1	−2.1
E·[Tyr-ATP]‡ [d]	5.40	9.40	1.2	−5.4	0.2
E·Tyr·ATP (no synergism)[b,e]	−10.07	−10.24	0.1	2.4	−2.3

[a] G and G_o are the free energies for the complexes with substrates of wild-type and *K230A/K233A/T234A* triple mutant, respectively, relative to the free energy of the uncomplexed parent enzyme. The standard states are 1 M. [b] Energies are in kcal mol^{-2}. [c] Energies are in kcal mol^{-3}. [d] Energies are in kcal mol^{-1}. [e] The free energy changes for the E·Tyr·ATP complex in the absence of synergism between the tyrosine and ATP substrates were calculated by replacing the K'_{ATP} with K_{ATP}, where K_{ATP} is the dissociation constant for ATP in the absence of enzyme-bound tyrosine.

First & Fersht, 1993a,c). As mutation of the mobile loop does not alter the stability of the E·Tyr complex, it is not possible to evaluate either the strength or existence of pairwise and ternary couplings between K230, K233, and T234 for this complex.

Dissection of the Mobile Loop's Effect on the Stability of the E·ATP Complex. As indicated in eq 4, the free energy change associated with mutation of the mobile loop ($G_n - G_o$) can be separated into terms corresponding to (1) the free energy changes associated with the addition of each wild-type side chain to the *K230A/K233A/T234A* triple mutant ($\sum\Delta G_1$), and (2) pairwise and higher order coupling terms associated with the interactions between the wild-type side chains (e.g., $\sum\Delta^2 G_{int}$ and $\Delta^3 G_{int}$). The contribution of each of these terms towards the net effect of the mobile loop is discussed below for the E·ATP, E·Tyr·ATP, and E·[Tyr-ATP]‡ complexes.

Comparison of K_{ATP} values for K230/K233/T234 with those of the *K230A/K233A/T234A* triple mutant indicates that the mobile loop has only a small effect on the binding of ATP when tyrosine is not bound to the enzyme (Table 1). This results in a small difference in the stabilities of the E·ATP complexes for these two species (shown in Table 2, G and G_o represent the relative stabilities of the E·Tyr·ATP complexes for the wild-type and *K230A/K233A/T234A* enzymes). Despite the small net difference in the free energies for the wild-type enzyme and the *K230A/K233A/T234A* triple mutant, however, dissection of this net free energy difference into its individual components indicates that it is composed of larger, offsetting free energy changes (Table 2). The free energy cycles used to calculate the individual components of the net free energy change are shown in Figure 5. The six cycles shown in Figure 5 represent the six faces of a triple mutant cube (Figure 2) for the E·ATP complex. To calculate the $\sum\Delta G_1$ term (0.9 kcal/mol, Table 2), the individual ΔG_1 values associated with the addition of each wild-type side chain to the *K230A/K233A/T234A* triple mutant (the relevant ΔG_a and ΔG_b values in Figure 5) are determined and the sum of these terms is calculated. $\Delta^2 G_{int}$ values are calculated from the difference between the free energy changes corresponding to processes located on opposite sides of the free energy cycle (e.g., $\Delta G_d - \Delta G_a$ in cycle A). The $\sum\Delta^2 G_{int}$ term (1.9 kcal/mol in Table 2) is calculated from the sum of the $\Delta^2 G_{int}$ values determined from double mutant cycles in which the *K230A/K233A/T234A* triple mutant is the reference protein (Figure 5, cycles A, C, and E). Finally, the $\Delta^3 G_{int}$ term is the difference between $\Delta^2 G_{int}$ values calculated from any pair of free energy cycles located on opposing sides of the triple mutant cube shown in Figure 2 (e.g., in Figure 5 $\Delta^2 G_{int}$ for cycle B − $\Delta^2 G_{int}$ for cycle A). As mentioned previously, negative free energy values for a particular term indicate a stabilizing effect in the wild-type enzyme, whereas positive free energy values indicate a destabilizing effect. Thus, destabilization of the E·ATP complex by the $\sum\Delta G_1$ and $\sum\Delta^2 G_{int}$ terms (by a total of 2.4 kcal/mol) is offset by the −2.1 kcal/mol of (stabilizing) free energy associated with the ternary coupling term, $\sum\Delta^3 G_{int}$ (i.e., by the effect that the third wild-type side chain has on the coupling between the other two wild-type side chains).

Dissection of the Mobile Loop's Effect on the Stability of the E·Tyr·ATP Complex. Comparison of the K'_{ATP} values for the wild-type and the *K230A/K233A/T234A* enzymes indicates that, in the wild-type enzyme, the presence of a

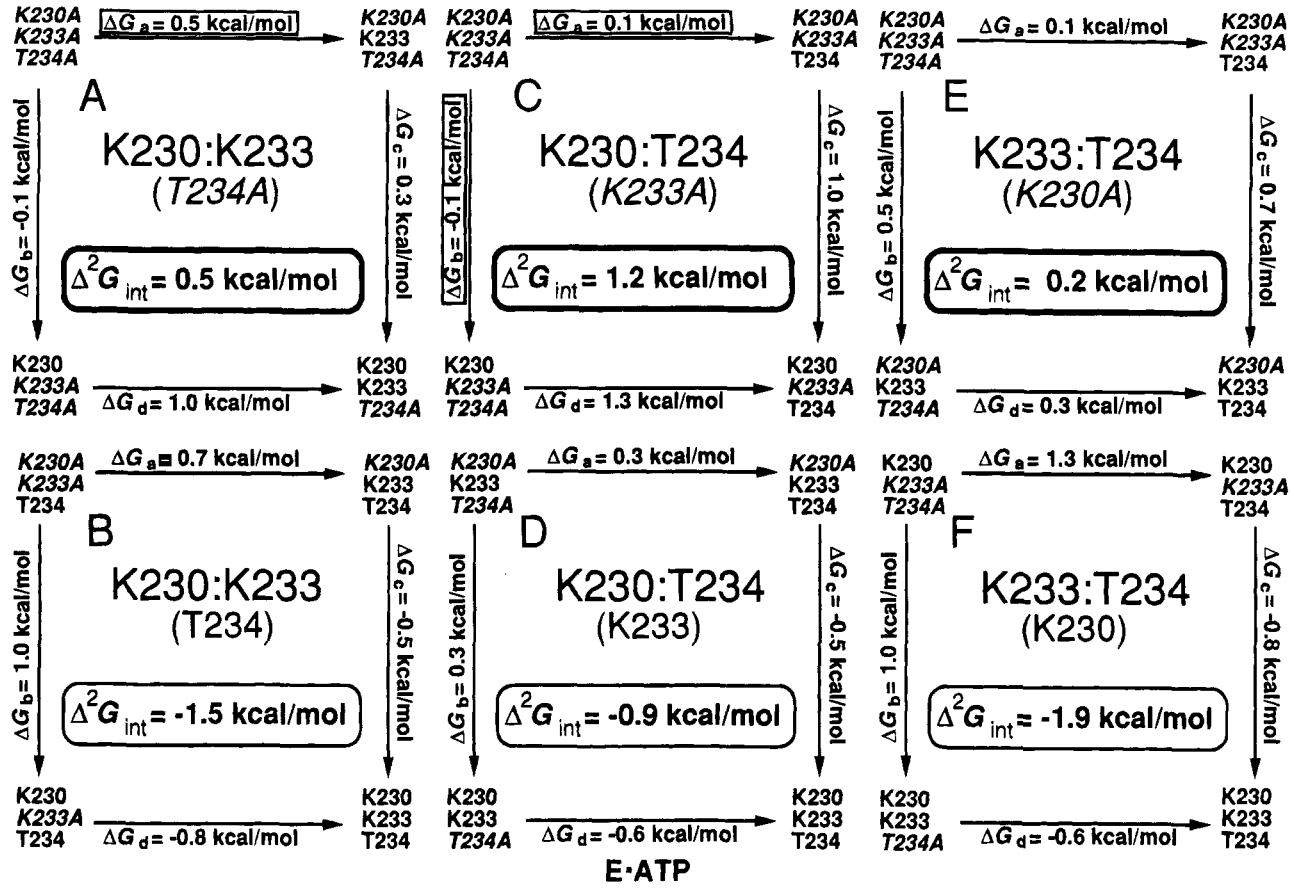

FIGURE 5: Pairwise couplings between the side chains of K230, K233, and T234 relative to alanine for the E·ATP complex. Pairs of cycles (A + B, C + D, E + F) represent the same pairwise couplings but in the context of a different amino acid side chain in the third position (alanine for cycles A, C, and E; wild type for cycles B, D, and F). The amino acid side chains involved in pairwise coupling are shown in the center of each cycle, with the identity of the third amino acid side chain underneath, in parentheses. $\Delta G_{a-d} = G_{E\cdot ATP}$(species 2) − $G_{E\cdot ATP}$(species 1), where species 1 is the enzyme containing the larger number of alanine mutations (e.g., for ΔG_a = 0.7 kcal/mol in cycle A, species 1 is *K230A/K233A/T234A* and species 2 is *K230A*/K233/T234A). Δ^2G_{int} for each cycle is calculated by subtraction of the changes in free energy for opposing sides of the cycle (e.g., $\Delta^2G_{int} = \Delta G_d - \Delta G_a = -0.3$ kcal/mol for cycle A).

functional mobile loop decreases the affinity of the E·Tyr complex for ATP by 50-fold. This destabilizes the E·Tyr·ATP complex by 2 kcal/mol (Table 2, $G - G_o$). This is similar to the effect that deletion of the mobile loop has on the stability of the E·Tyr·ATP complex (First & Fersht, 1993c). As was the case for the E·ATP complex, dissection of the net free energy difference for the E·Tyr·ATP complex into its component parts indicates that it is composed of larger free energy changes, with the Δ^3G_{int} term partially offsetting the $\sum\Delta G_1$ and $\sum\Delta^2G_{int}$ terms (Table 2). The free energy cycles used to calculate the individual components of the net free energy change for the E·Tyr·ATP complex are shown in Figure 6. The main component of the $\sum\Delta G_1$ term is the free energy change associated with the introduction of the K233 side chain into the *K230A/K233A/T234A* triple mutant which destabilizes the E·Tyr·ATP complex by 2 kcal/mol (Figure 6, ΔG_a value in cycle A). The net effect of the Δ^2G_{int} values ($\sum\Delta^2G_{int}$ in Table 2) is to destabilize the E·Tyr·ATP complex by 2.1 kcal/mol. This is primarily due to coupling between amino acids K230 and T234 destabilizing the E·Tyr·ATP complex by 2.5 kcal/mol relative to alanine (Figure 6, cycle C). The combined effect of the $\sum\Delta G_1$ and $\sum\Delta^2G_{int}$ terms is to destabilize the E·Tyr·ATP complex by 4.3 kcal/mol. This destabilization is partially offset by the ternary coupling between the K230, K233, and T234 side chains which stabilizes the E·Tyr·ATP complex by −2.1 kcal/mol (Table 2, Δ^3G_{int}). Thus, the net effect of the mobile loop on the E·Tyr·ATP complex is to destabilize it by 2.2 kcal/mol.

Dissection of the Mobile Loop's Effect on the Stability of the E·[Tyr-ATP]‡ Transition State Complex. Comparison of the forward rate constants for the wild-type and *K230A/K233A/T234A* enzymes indicates that the mobile loop increases the rate of the reaction by five orders of magnitude (Table 1). This agrees well with the results obtained when the entire mobile loop is deleted (Fersht & Fersht, 1993c). Comparison of the G and G_o values indicates that the net effect of the mobile loop is to stabilize the E·[Tyr-ATP]‡ complex by 4 kcal/mol (Table 2). Stabilization of the E·[Tyr-ATP]‡ complex is entirely due to the $\sum\Delta^2G_{int}$ term. As indicated in Figure 7 (cycles A, C, and E), all three pairwise couplings between the K230, K233, and T234 side chains stabilize the E·[Tyr-ATP]‡ complex with approximately equal magnitude (−1.5 to −2.1 kcal/mol). These pairwise couplings are slightly offset by the ΔG_1 terms, primarily by the introduction of the K233 side chain into the *K230A/K233A/T234A* triple mutant (Figure 7, ΔG_a in cycle A). There is no ternary coupling between the three wild-type amino acid side chains (e.g., the difference between the Δ^2G_{int} values for cycles A and B in Figure 7 is negligible).

Contribution of the Mobile Loop to the Stability of the E·Tyr-AMP·PPi and E·Tyr-AMP Complexes. As it is not

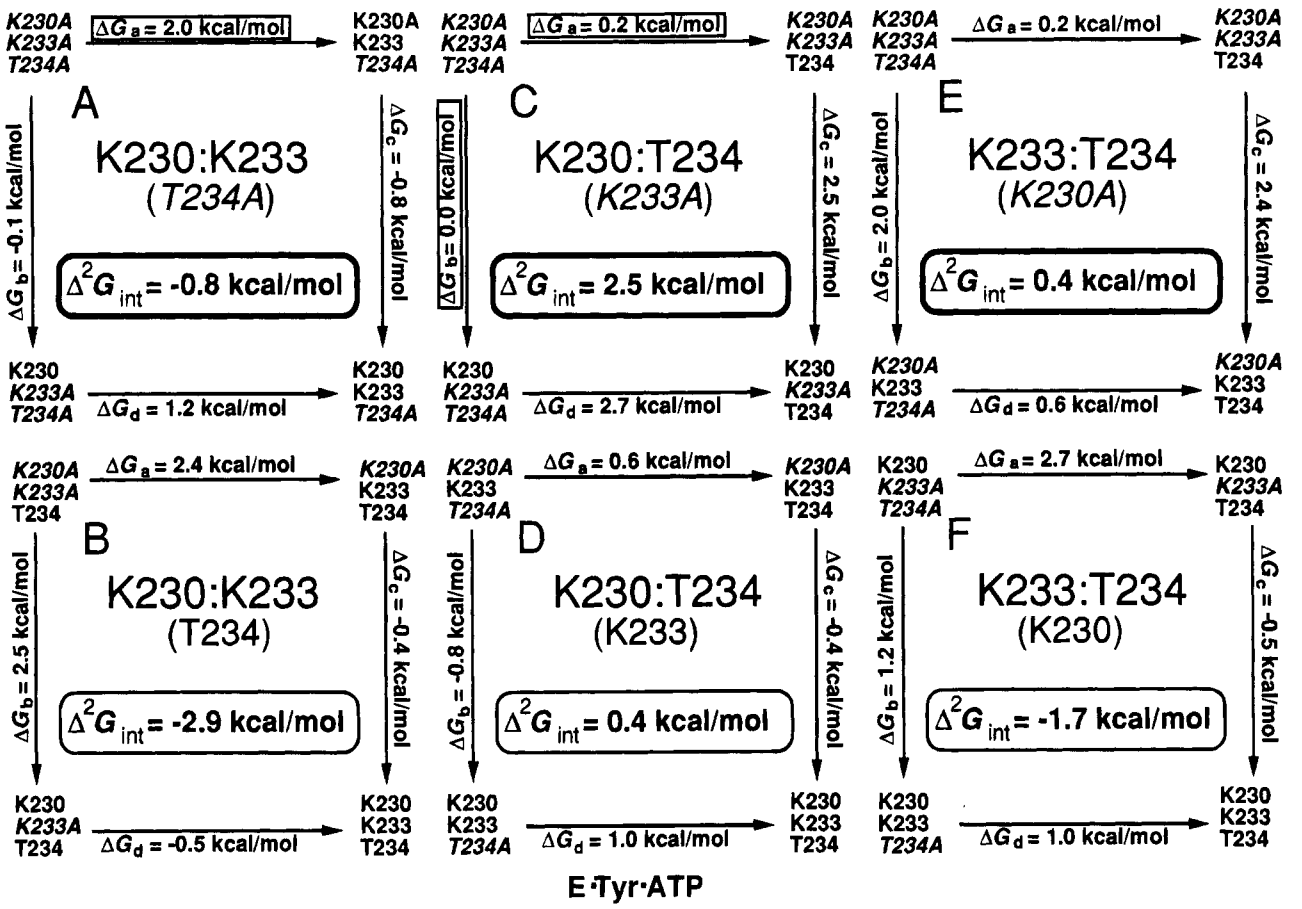

FIGURE 6: Pairwise couplings in the E·Tyr·ATP complex. See Figure 4 legend for an explanation of the formalism used.

possible to measure pyrophosphorolysis above the background rate for any of the multiple alanine mutants except the *K230A*/K233/*T234A* double mutant, it is impossible to quantify fully the effects that coupling between K230, K233, and T234 have on the stability of the E·Tyr-AMP·PP_i and E·Tyr-AMP complexes. The effect of pairwise coupling between K230 and T234 on the stability of these complexes has been demonstrated previously (First & Fersht, 1993a). As demonstrated by the pairwise and ternary couplings in the E·Tyr·ATP complex, it is impossible to determine the net effect of the mobile loop on the basis of one pairwise coupling term. The presence of coupling between K230 and T234 does indicate, however, that the mobile loop is able to affect the stabilities of the E·Tyr-AMP·PP_i and E·Tyr-AMP complexes.

Disruption of the Synergistic Coupling between the Tyrosine and ATP Substrates by the Mobile Loop. Comparison of the dissociation constants for ATP indicates that mutations in tyrosyl-tRNA synthetase that render the loop nonfunctional (e.g., the *K230A/K233A/T234A* triple mutant) increase the ATP binding affinity of the enzyme 50-fold compared with that of the wild-type enzyme (Table 1). This contrasts sharply with the situation that exists when tyrosine is not bound to the enzyme. In this latter case, the affinity of the *K230A/K233A/T234A* triple mutant for ATP is decreased 20-fold, whereas the affinity of the wild-type enzyme for ATP shows only a slight increase (Table 1). As a result, in the absence of enzyme-bound tyrosine, the affinities of the wild type and *K230A/K233A/T234A* triple mutant enzymes for ATP are within 2-fold of each other. Comparison of the K_{Tyr} values indicates that the mobile loop does not interact directly with the tyrosine substrate (Table 1). Thus, in the absence of a functional mobile loop, there is synergistic coupling between the ATP and tyrosine substrates. This synergism is disrupted by the interaction of the mobile loop with the ATP substrate (Table 1). To elucidate the mechanism responsible for the disruption of synergism between the ATP and tyrosine substrates, a triple mutant free energy cube was constructed which corresponds to an E·Tyr·ATP complex in which no synergism exists between the tyrosine and ATP substrates, irrespective of the functionality of the mobile loop. In other words, the K'_{ATP} term is replaced by K_{ATP} when calculating the relative stabilities for the wild-type and mutant enzymes. The net contributions of each free energy term for this triple mutant cube are compared with those of the actual E·Tyr·ATP complex (Table 2). It can be seen from this comparison that, in contrast to the actual E·Tyr·ATP complex, in the absence of synergism between the tyrosine and ATP substrates, there is little difference between the relative stabilities of the wild type (G) and *K230A/K233A/T234A* triple mutant (G_o) enzymes. This is due to a 2.0 kcal/mol decrease in the $\Sigma\Delta G_i$ term for the hypothetical E·Tyr·ATP complex in which synergism between tyrosine and ATP is absent. Table 3 illustrates in greater detail the effects of removing the synergistic binding of tyrosine and ATP. Comparison of ΔG_i values for the addition of each individual amino acid indicates that only the addition of the K233 side chain significantly disrupts the synergism between the tyrosine and ATP substrates. Analysis of the pairwise couplings indicates that although the net difference between the $\Sigma\Delta^2G_{int}$ terms is negligible, this is due to the effect of coupling between K230 and K233

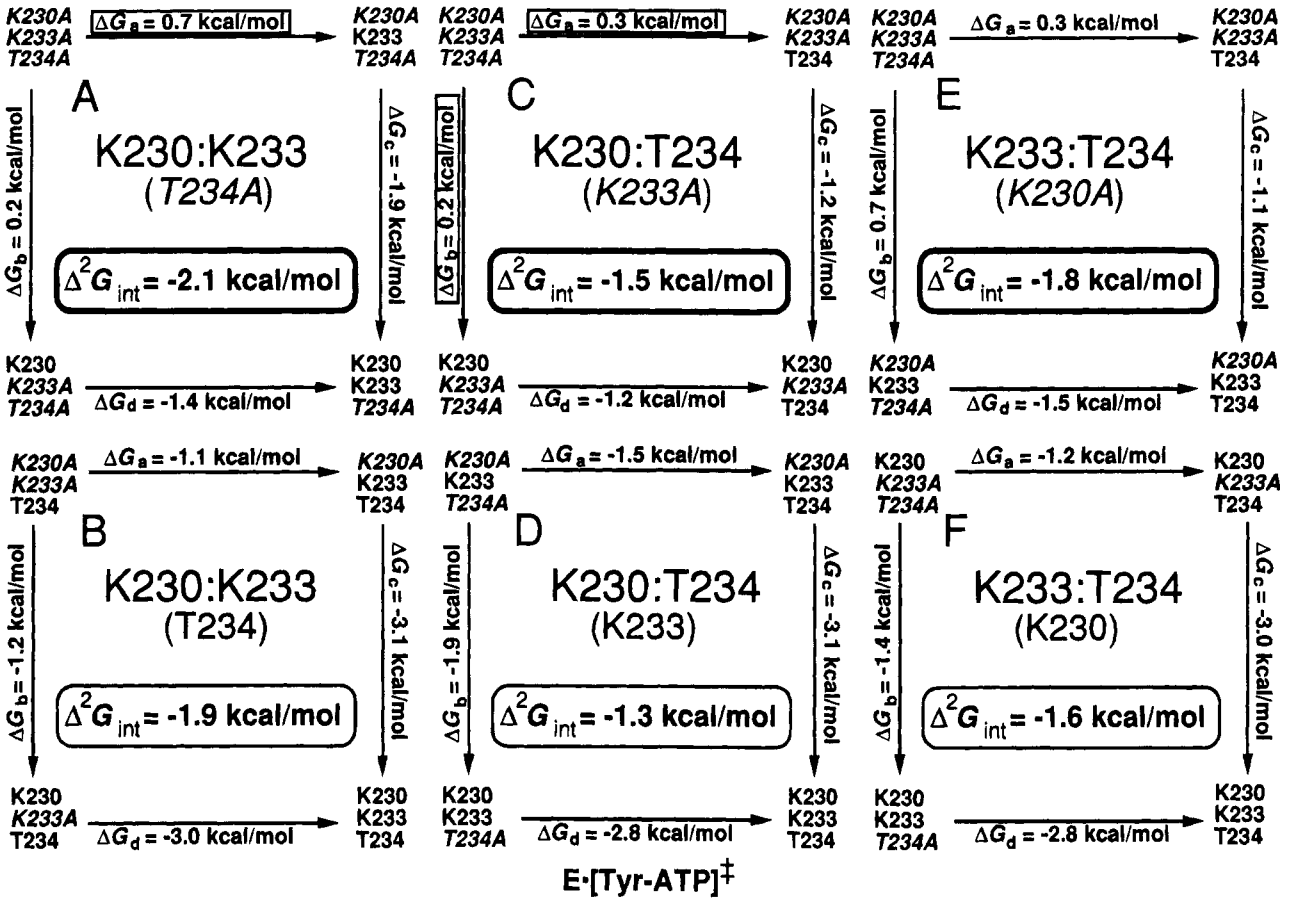

FIGURE 7: Pairwise couplings in the E·[Tyr-ATP]‡ complex. See Figure 4 legend for an explanation of the formalism used.

Table 3: Effects of Tyrosine on the Components of the $\sum\Delta G_1$, Δ^2G_{int}, and $\sum\Delta^3G_{int}$ Terms for the E·Tyr·ATP Complex[a]

amino acid	$\Delta(\sum\Delta G_1)$[a]
K230	0.3
K233	1.5
T234	0.2
pairwise interaction	$\Delta(\sum\Delta^2G_{int})$[a]
K230:K233	−1.3
K230:T234	1.2
K233:T234	0.0
ternary interaction	$\Delta(\Delta^3G_{int})$[a]
K230:K233:T234	0.2

[a] The effects of tyrosine were determined by calculating the ΔG_1, Δ^2G_{int}, and Δ^3G_{int} values for two triple mutant cubes: cube 1 representing the E·Tyr·ATP complex in the presence of synergistic coupling between the ATP and tyrosine substrates and cube 2 representing the E·Tyr·ATP complex in the absence of synergism between the substrates. Free energy values were calculated from the equations $G = -RT \ln K_{Tyr}K'_{ATP}$ for the first cube and $G = -RT \ln K_{Tyr}K_{ATP}$ for the second cube. Differences in free energy changes [i.e., $\Delta(\Delta G_1)$, $\Delta(\Delta^2G_{int})$, and $\Delta(\Delta^3G_{int})$] are calculated by subtracting the free energy changes calculated for cube 1 from those of cube 2. All energies are kcal mol^{-2}.

offsetting those between K230 and T234. Interestingly, it is the coupling between K230 and T234 that disrupts the synergism between tyrosine and ATP (by 1.2 kcal/mol) indicating that, in the wild-type enzyme, all three amino acid side chains are involved in disrupting the synergism between tyrosine and ATP. Finally, the difference between the ternary coupling terms is not affected by the synergism between tyrosine and ATP.

As implied by comparison of the two triple mutant cubes for the E·Tyr·ATP complexes, the tyrosine substrate can be considered explicitly as a fourth variable (where the identities of the amino acid at positions 230, 233, and 234 in tyrosyl-tRNA synthetase are the first three variables). Graphically, this can be pictured as a four-dimensional hypercube (Horovitz & Fersht, 1990) in which a triple mutant cube corresponding to the actual E·Tyr·ATP complex (i.e., one in which tyrosine is present at saturating tyrosine concentrations) is surrounded by a triple mutant cube corresponding to the hypothetical E·Tyr·ATP complex in which there is no synergism between the tyrosine and ATP substrates (i.e., the outer triple mutant cube is identical to the inner triple mutant cube except that the concentration of tyrosine is at least 10-fold lower than the value of its dissociation constant). The vertices of the outer cube are connected to the vertices of the inner cube by arrows pointing toward the inner cube. In other words, the "wild-type" complex is considered to be the K230/K233/T234 enzyme at saturating tyrosine concentrations.

Application of eq 4 to the case of a four-dimensional hypercube permits dissection of the free energy changes for the E·Tyr·ATP complex into its individual components. This is analogous to the analyses shown in Table 2, except that now couplings between the mobile loop and the tyrosine substrate are explicitly considered. When the tyrosine concentration is included as an explicit variable in the E·Tyr·ATP complex, there is little difference in the free energy of the wild-type enzyme and that of the quadruple mutant (*K230A/K233A/T234A*/0.5 μM tyrosine, $G - G_o = 0.2$). Analysis of the individual components, however,

indicates this is due to larger free energy differences in the $\sum\Delta G_1$ (−1.3 kcal/mol), $\sum\Delta^2 G_{int}$ (4.4 kcal/mol), and $\sum\Delta^3 G_{int}$ (−2.6 kcal/mol) terms which essentially offset each other. Comparison with Table 2 shows that considering tyrosine as an explicit variable substantially alters the net values of the $\sum\Delta G_1$ and $\sum\Delta^2 G_{int}$ terms, consistent with the hypothesis that tyrosine is coupled to both the ATP substrate and the mobile loop. In addition, analysis of the individual free energy changes that make up the $\sum\Delta^3 G_{int}$ term indicates that ternary interactions involving tyrosine contribute both positive and negative $\Delta^3 G_{int}$ values. No significant quaternary coupling is observed between the four variables in the E·Tyr·ATP complex.

DISCUSSION

The Mobile Loop Uses ATP Binding Energy to Stabilize the E·[Tyr-ATP]‡ Transition State Complex. In the absence of a functional mobile loop, synergism is observed between the tyrosine and ATP substrates (Table 1, K_{ATP} vs. K'_{ATP} for the *K230A/K233A/T234A* mutant). As this synergism is not observed in the wild-type enzyme, one function of the mobile loop must be to disrupt the synergism between tyrosine and ATP in the E·Tyr·ATP complex. Moreover, mutation of the mobile loop destabilizes the E·[Tyr-ATP]‡ transition state complex (Table 2; First & Fersht, 1993c) indicating that in the wild-type enzyme stabilization of the transition state complex occurs at the expense of the preceding E·Tyr·ATP complex.

Three lines of evidence indicate that the transfer of binding energy from the E·Tyr·ATP complex to the transition state complex occurs through the interaction of the mobile loop with the ATP substrate. First, evidence in this and previous investigations indicates that amino acids K230, K233, and T234 in the mobile loop interact directly with the phosphate groups of ATP (Fersht et al., 1988; First & Fersht, 1993a,b,c). Second, the initial binding of the tyrosine substrate is unaffected by the presence or absence of a functional mobile loop, indicating the tyrosine substrate does not interact with the mobile loop in the absence of ATP (Table 1; First & Fersht, 1993c). Third, the X-ray crystal structure of the tyrosyl-tRNA synthetase−tyrosine complex suggests that the mobile loop and tyrosine substrate do not directly interact with each other (Brick & Blow, 1987; Brick et al., 1989). One consequence of the disruption of coupling between the tyrosine and ATP substrates by the mobile loop is that amino acids K230, K233, and T234 are in effect coupled to the tyrosine substrate through their interactions with ATP. The net effect of this coupling between the mobile loop and the tyrosine substrate (i.e., the disruption of synergism between the tyrosine and ATP substrates) is to destabilize the E·Tyr·ATP complex by 2 kcal/mol.

The hypothesis that the coupling between the tyrosine substrate and the mobile loop is mediated by the phosphate groups of the ATP substrate is consistent with previous observations made by Blanquet and co-workers for methionyl-tRNA synthetase (Blanquet et al., 1975a,b; Hyafil et al., 1976; Fayat et al., 1977; Mechulam et al., 1991). Whereas no synergism is observed between methionine and ATP in wild-type methionyl-tRNA synthetase, when methionine is replaced by an analogue lacking the carboxylate group (methioninol) a strong synergism is observed between the methionine analogue and ATP, suggesting that the amino group of methionine interacts with the phosphate groups of ATP. The presence of similar synergistic couplings in both methionyl- and tyrosyl-tRNA synthetase suggests that this is a general feature of the catalytic mechanism for the class I aminoacyl synthetases. It has been postulated that when methionine is present, the free energy gained through this synergism counteracts the electrostatic repulsion between the methionyl carboxyl group and the phosphoryl groups of ATP that result when the two substrates are properly aligned in the active site of the enzyme. This suggests a mechanism in which the mobile loop positions the phosphate groups of the ATP substrate such that the reaction of the carboxyl group of the amino acid substrate with the γ-phosphate group of ATP is enhanced.

The Energetics of Tyrosyl Adenylate Formation Are Consistent with the Transition State Model Proposed by Leatherbarrow et al. (1985). On the basis of the X-ray crystal structure of the tyrosyl-tRNA synthetase·Tyr-AMP intermediate, Leatherbarrow et al. (1985) proposed a model for catalysis in tyrosyl-tRNA synthetase in which binding energy is used to stabilize the transition state relative to the initial state of the reaction. In this model, it is proposed that the γ-phosphate group of ATP is initially surrounded by solvent but, on formation of the transition state complex, moves into a binding pocket on the enzyme. This model correctly predicted the involvement of T40 and H45 in stabilizing (relative to the free enzyme) the E·[Tyr-ATP]‡ transition state complex but not the E·Tyr·ATP intermediate. This model is also consistent with the evidence presented in this paper, which indicates that the mobile loop uses the energy for binding ATP to stabilize the E·[Tyr-ATP]‡ transition state complex relative to the free enzyme.

Recently, a variation of the model proposed by Leatherbarrow et al. has been postulated (Perona et al., 1993). In this variation, which is based on the X-ray crystal structure of the glutaminyl-tRNA synthetase·$tRNA^{Gln}$·ATP ternary complex, it is assumed that the enzyme initially fixes the position of the pyrophosphate moiety of ATP (i.e., the configuration of the phosphate groups does not significantly change on conversion of the E·AA·ATP complex to the E·[AA-ATP]‡ complex). Although the kinetic evidence presented here does not strictly rule out this variation for the catalytic mechanism of tyrosyl-tRNA synthetase, changes in the observed interactions between the mobile loop and the phosphate groups on ATP in going from the E·Tyr·ATP intermediate to the E·[Tyr-ATP]‡ transition state complex suggest that these phosphates do undergo a conformational change during formation of the transition state complex. It should be noted that several differences appear to exist between the active sites of tyrosyl-tRNA synthetase and glutaminyl-tRNA synthetase. Although the homologous lysines, K233 of tyrosyl-tRNA synthetase and K270 of glutaminyl-tRNA synthetase, appear to play similar roles in catalysis, the precise roles of the two histidine residues in the HIGH regions of the enzymes appears to be different for each of the enzymes. In addition, whereas in tyrosyl-tRNA synthetase K82 and R86 have been implicated in stablilizing the phosphate groups of ATP, no homologous residues for K82 and R86 have been identified in the glutaminyl-tRNA synthetase. These differences may reflect real differences in the catalytic mechanisms of the two enzymes (glutaminyl-tRNA synthetase, for example, requires tRNA to form the aminoacyl adenylate species, whereas

tyrosyl-tRNA synthetase does not). Alternatively, it may reflect differences in the complexes on which the transition state models are based (i.e., the Leatherbarrow et al. model is based on the X-ray crystal structure of the tyrosyl-tRNA synthetase•Tyr-AMP complex, whereas the variation proposed by Perona et al. is based on the glutaminyl•$tRNA^{Gln}$•ATP ternary complex). Finally, it should be emphasized that although the mechanistic details proposed by Leatherbarrow et al. (1985) and Perona et al. (1993) differ slightly, both models are in agreement that it is the use of binding energy to stabilize the transition state of the reaction (relative to the ground state) which is responsible for the catalytic effects of the two enzymes.

The Contribution of Coupling Energies to the Stability of Each Step in the Reaction Pathway. The mobile loop has previously been shown to have no effect on the stability of the E•Tyr complex (First & Fersht, 1993c). This is confirmed by the findings of this investigation. For the E•Tyr•ATP complex, previous investigation has shown that the net effect of the mobile loop is to destabilize this complex by 2 kcal/mol, decreasing the free energy difference between the E•Tyr•ATP and E•[Tyr-ATP]‡ complexes (First & Fersht, 1993c). The present investigation delineates the energetics of this destabilization. Specifically, the net destabilization of the E•Tyr•ATP complex by 2 kcal/mol results from a balance between the destabilizing effects of both the K233 side chain and the pairwise coupling between K230 and T234, and the stabilizing effect of the ternary coupling between all three side chains.

In the E•[Tyr-ATP]‡ complex, the net effect of the mobile loop is to stabilize this complex by 4.0 kcal/mol (First & Fersht, 1993c). Previous investigations have implicated K230, K233, and T234 as the amino acids in the mobile loop that are responsible for this stabilization (Fersht et al., 1988; First & Fersht, 1993a). In addition, X-ray crystallographic analysis of the glutaminyl-tRNA synthetase indicates that K270, which is homologous to K233 in tyrosyl-tRNA synthetase, is within hydrogen bonding distance of oxygen atoms associated with the α- and γ-phosphate groups of ATP, as well as the bridging oxygen between the α- and β-phosphate groups. This agrees with the role proposed for K233 by Fersht et al. (1988) on the basis of site-directed mutagenesis and enzyme kinetics. The X-ray crystal structure of glutaminyl-tRNA synthetase complexed with ATP and $tRNA^{Gln}$ also indicates that the Mg^{2+} ion is ligated to the β- and γ-phosphate groups of ATP, in agreement with the results of the kinetic analysis of tyrosyl-tRNA synthetase using phosphorothioate ATP analogues (Garcia et al., 1990).

In contrast to the E•Tyr•ATP complex, conflicting effects and interactions are minimized in the transition state complex. This leaves the three stabilizing pairwise interactions between the K230, K233, and T234 side chains, each of which is of similar magnitude (-1.5 to -2.1 kcal/mol). The minimization of conflicting effects is particularly apparent on comparison of the ΔG_1 terms for the E•Tyr•ATP and E•[Tyr-ATP]‡ complexes. Whereas in the E•Tyr•ATP complex the introduction of a single amino acid side chain (K233) has substantial effects on the stability of the complex (2.0 kcal/mol), in the E•[Tyr-ATP]‡ complex none of the ΔG_1 terms is larger than 0.7 kcal/mol.

The observation that the removal of any one of the three amino acid side chains disrupts pairwise couplings with the other two amino acids suggests that the mobile loop adopts a highly constrained conformation in the E•[Tyr-ATP]‡ complex. This hypothesis is supported by the X-ray crystal structure for the glutaminyl-tRNA synthetase•$tRNA^{Gln}$•ATP complex, in which the mobile loop is found to adopt a well-ordered conformation (Perona et al., 1993). It should be noted that the conformations of the mobile loop in the X-ray crystal structures of the tyrosyl-tRNA synthetase•Tyr-AMP complex and the glutaminyl-tRNA synthetase•$tRNA^{Gln}$•ATP complex are substantially different (Brick et al., 1989; Perona et al., 1993), although this may result from the different ligation states of the two enzymes rather than their differing amino acid specificities. In addition, as has been previously observed, the mobile loop in tyrosyl-tRNA synthetase displays a high degree of conformational flexibility and may adopt a conformation in the E•[Tyr-ATP]‡ complex that differs from that seen in the crystal structure (Fersht et al., 1988; Perona et al., 1993). This is consistent with the results presented here, as the tight pairwise coupling between the K230, K233, and T234 side chains provides a rationale for the conservation of the KMSKS signature sequence, implying that the mobile loop adopts a similar conformation in the E•[Tyr-ATP]‡ transition state complex for all class I aminoacyl-tRNA synthetases.

Amino Acids K230, K233, and T234 Form a Subnetwork of Interacting Amino Acids Which Act in Concert To Catalyze the Formation of the Tyrosyl Adenylate Intermediate. It is apparent from Tables 2 and 3 that coupling between K230, K233, and T234 plays a significant part in determining whether the mobile loop stabilizes or destabilizes a particular complex in the reaction pathway. While this is most apparent in the E•[Tyr-ATP]‡ complex, where the pairwise coupling term entirely accounts for stabilization of this complex, pairwise and higher order coupling effects are seen at all steps in which the mobile loop participates in the catalytic reaction. It is interesting to note that, whereas in the steps preceding formation of the transition state complex the coupling terms generally offset one another, stabilization of the transition state complex is in part achieved by minimizing the unfavorable interactions between the K230, K233, and T234 side chains.

The energetic analysis of coupling energies presented here provides an excellent example of the influence that neighboring amino acid side chains exert on one another and, as previously observed by others (Carter et al., 1984; Wells, 1990; Steyaert & Wyns, 1993), illustrates the limitations of using single mutants in analyzing structure-function relationships in proteins. The tight energetic coupling seen between K230, K233, and T234 is reminiscent of the couplings found between D32, H64, and S221 in subtilisin (Carter & Wells, 1988, 1990) and between H40, E58 and H92 in ribonuclease T_1 (Steyaert & Wyns, 1993). In each of these enzymes, mutation of one member of the trio alters the catalytic effect of the other members. The couplings observed in tyrosyl-tRNA synthetase are unique, however, in that they all occur within a single structural element, the mobile loop. This has permitted the net effect of the loop (determined by deletion of the mobile loop) to be dissected into its component parts (i.e., the effect of isolated amino acid side chains + the effect of pairwise couplings + the effect of ternary coupling) to elucidate the contributions of each part in the total effect of the mobile loop on the catalytic mechanism. In other words, within the mobile loop, all of the different side chain environments that affect catalysis

have been investigated. This does not, of course, exclude additional couplings with other parts of the enzyme. For example, it is possible that the KMSKS mobile loop interacts with the conserved HIGH sequence in the aminoacyl-tRNA synthetases. All significant effects of energetic coupling within the mobile loop have, however, been quantified.

It should be emphasized that higher order coupling terms (i.e., Δ^2G_{int} and Δ^3G_{int}) do not necessarily measure direct interactions between amino acid side chains. Rather, non-additive coupling terms can result from several different types of effects including (1) direct effects, where amino acid side chains are in direct contact with each other, (2) indirect "environmental" effects, where the amino acid side chains are coupled through intermediary amino acids or through their interactions with substrate molecules, (3) gross structural effects, where replacement of one amino acid side chain disrupts the tertiary structure of the protein, indirectly affecting the ability of active site amino acids to participate in catalysis, and (4) indirect "conformational" effects, where replacement of an amino acid side chain affects the stability of a particular conformation of the protein, altering the ability of active-site amino acids to participate in the catalytic mechanism (i.e., an amino acid side chain, *j*, which stabilizes a conformation that is necessary for catalysis, will produce Δ^2G_{int} terms which reflect the coupling between the amino acid and active-site amino acids since addition of the side chain *j* enhances the probability of the active site amino acids being in the correct conformation to catalyze the reaction). In the mobile loop mutants, gross structural effects are unlikely to be the cause of the higher order coupling that is observed in the E·TyrATP and E·[Tyr-ATP]‡ complexes. The evidence for this is as follows: (1) on the basis of X-ray crystallography, all three amino acids investigated in this paper, K230, K233, and T234, occur in a flexible surface loop (Brick et al., 1989), (2) the binding of the tyrosine substrate is unaffected in these mutants, indicating that no gross structural changes have occurred, and (3) elution of mutant enzymes from an FPLC Mono-Q column is similar to that of the wild-type enzyme. In addition, deletion of the entire loop does not appear to induce any gross structural changes by the above criteria. Thus, as far as the tertiary structure of tyrosyl-tRNA synthetase is concerned, the mobile loop appears to be superfluous. The coupling effects observed are, therefore, due either to direct interactions or to indirect interactions that are either environmental or conformational in nature.

Summary and Conclusions. In the absence of a functional mobile loop, there is synergistic coupling between the ATP and tyrosine substrates. The mobile loop disrupts this synergism, destabilizing the E·TyrATP intermediate by 2 kcal/mol but stabilizing the subsequent E·[Tyr-ATP]‡ transition state complex. Stabilization of the E·[Tyr-ATP]‡ transition state complex is entirely due to pairwise couplings between the K230, K233, and T234 side chains, suggesting the mobile loop is in a highly constrained conformation in this complex. It should be emphasized that neither the mechanism by which the E·TyrATP intermediate is destabilized nor the high degree of synergism between the K230, K233, and T234 side chains that is required to stabilize the E·[Tyr-ATP]‡ transition state complex could have been elucidated from analysis of single mutants alone. Instead, it was necessary to use multiple mutant free energy cycles both to identify these essential features and to quantify the network of interactions that are responsible for the mobile loop's participation in the catalytic mechanism of tyrosyl-tRNA synthetase.

APPENDIX

The free energies of coupling for the various intermediate and transition state complexes are shown below. G_2 is defined in eq 4. In each case, the reference protein indicates the most highly mutated species in the free energy cycle being analyzed, $G_{2(expt)}$ represents the actual free energy of the least mutated protein in the cycle relative to the unligated state of the enzyme, $G_{o(add)}$ represents the free energy that the least mutated protein in the cycle would have (relative to the unligated state of the enzyme) if there is no coupling (i.e., if the free energy of coupling is zero), Δ^2G_{int} is the

Table A1: Free Energies of Coupling in the E·ATP Complex

coupling analyzed	unchanged amino acid	reference protein	$G_{2(expt)}$ (kcal/mol)	$G_{2(add)}$ (kcal/mol)	Δ^2G_{int} (kcal/mol)	effect of coupling on the stability of the E·ATP complex[a]
K230:K233	(T234)	K230/K233/T234	−3.35 ± 0.05	−2.0 ± 0.2	−1.4 ± 0.2	stabilizing
K230:K233	(*T234A*)	*K230A/K233A*/T234	−2.79 ± 0.06	−3.1 ± 0.3	0.3 ± 0.1	negligible
K230:T234	(K233)	*K230A*/K233/*T234A*	−3.35 ± 0.05	−2.7 ± 0.1	−0.7 ± 0.2	stabilizing
K230:T234	(*K233A*)	*K230A/K233A/T234A*	−2.53 ± 0.05	−3.5 ± 0.4	1.0 ± 0.4	destabilizing
K233:T234	(K230)	K230/*K233A/T234A*	−3.35 ± 0.05	−1.5 ± 0.4	−1.9 ± 0.4	stabilizing
K233:T234	(*K230A*)	*K230A/K233A/T234A*	−2.87 ± 0.07	−2.7 ± 0.3	−0.2 ± 0.3	negligible

[a] The stability of the E·ATP complex is measured for species 1 relative to the reference species.

Table A2: Free Energies of Coupling in the E·TyrATP Complex

coupling analyzed	unchanged amino acid	reference protein	$G_{2(expt)}$ (kcal/mol²)	$G_{2(add)}$ (kcal/mol²)	Δ^2G_{int} (kcal/mol²)	effect of coupling on the stability of the E·TyrATP complex[a]
K230:K233	(T234)	*K230A/K233A*/T234	−9.89 ± 0.07	−7.0 ± 0.1	−2.9 ± 0.2	stabilizing
K230:K233	(*T234A*)	*K230A/K233A/T234A*	−10.9 ± 0.2	−10.1 ± 0.3	−0.8 ± 0.3	stabilizing
K230:T234	(K233)	*K230A*/K233/*T234A*	−9.89 ± 0.07	−10.3 ± 0.2	0.4 ± 0.2	destabilizing
K230:T234	(*K233A*)	*K230A/K233A/T234A*	−9.37 ± 0.07	−11.9 ± 0.2	2.5 ± 0.2	destabilizing
K233:T234	(K230)	K230/*K233A/T234A*	−9.89 ± 0.07	−8.2 ± 0.2	−1.7 ± 0.3	stabilizing
K233:T234	(*K230A*)	*K230A/K233A/T234A*	−9.48 ± 0.08	−9.9 ± 0.2	0.4 ± 0.2	destabilizing

[a] The stability of the E·TyrATP complex is measured for species 1 relative to the reference species.

Table A3: Free Energies of Coupling for the E·[Tyr-ATP]‡ Complex

coupling analyzed	unchanged amino acid	reference protein	$G_{2(expt)}$ (kcal/mol^3)	$G_{2(add)}$ (kcal/mol^3)	Δ^2G_{int} (kcal/mol^3)	effect of coupling on the stability of the E·[Tyr-ATP]‡ complex[a]
K230:K233	(T234)	*K230A*/*K233A*/T234	5.4 ± 0.1	7.3 ± 0.2	−1.9 ± 0.2	stabilizing
K230:K233	(*T234A*)	*K230A*/*K233A*/*T234A*	8.2 ± 0.2	10.3 ± 0.4	−2.1 ± 0.4	stabilizing
K230:T234	(K233)	*K230A*/K233/*T234A*	5.4 ± 0.1	6.7 ± 0.3	−1.3 ± 0.3	stabilizing
K230:T234	(*K233A*)	*K230A*/*K233A*/*T234A*	8.4 ± 0.1	9.9 ± 0.3	−1.5 ± 0.3	stabilizing
K233:T234	(K230)	K230/*K233A*/*T234A*	5.4 ± 0.1	7.0 ± 0.3	−1.6 ± 0.3	stabilizing
K233:T234	(*K230A*)	*K230A*/*K233A*/*T234A*	8.5 ± 0.1	10.4 ± 0.2	−1.9 ± 0.3	stabilizing

[a] The stability of the E·[Tyr-ATP]‡ complex is measured for species 1 relative to the reference species.

Table A4: Free Energies of Coupling for the Binding of ATP at Saturating Tyrosine Concentrations

coupling analyzed	unchanged amino acid	reference protein	$G_{2(expt)}$ (kcal/mol)	$G_{2(add)}$ (kcal/mol)	Δ^2G_{int} (kcal/mol)	effect of coupling on the binding of ATP[a]
K230:K233	(T234)	*K230A*/*K233A*/T234	−3.17 ± 0.05	−0.6 ± 0.1	−2.6 ± 0.1	stabilizing
K230:K233	(*T234A*)	*K230A*/*K233A*/*T234A*	−4.1 ± 0.2	−3.3 ± 0.3	−0.8 ± 0.2	stabilizing
K230:T234	(K233)	*K230A*/K233/*T234A*	−3.17 ± 0.05	−3.7 ± 0.2	0.6 ± 0.1	destabilizing
K230:T234	(*K233A*)	*K230A*/*K233A*/*T234A*	−2.57 ± 0.08	−5.0 ± 0.2	2.4 ± 0.1	destabilizing
K233:T234	(K230)	K230/*K233A*/*T234A*	−3.17 ± 0.05	−1.4 ± 0.3	−1.8 ± 0.3	stabilizing
K233:T234	(*K230A*)	*K230A*/*K233A*/*T234A*	−3.15 ± 0.04	−3.2 ± 0.2	0.0 ± 0.2	negligible

[a] The effect of coupling on the binding of ATP is measured for species 1 relative to the reference species.

Table A5: Free Energies of Pairwise Coupling between Mobile Loop Mutants and the Tyrosine Substrate for the Binding of ATP

coupling analyzed	unchanged amino acids	reference protein (0.5 μM Tyr)	$G_{2(expt)}$ (kcal/mol)	$G_{2(add)}$ (kcal/mol)	Δ^2G_{int} (kcal/mol)	effect of coupling on the binding of ATP[a]
K230:Tyr	K233, T234	*K230A*/K233/T234	−3.17 ± 0.05	−3.7 ± 0.1	0.5 ± 0.1	destabilizing
K230:Tyr	*K233A*, T234	*K230A*/*K233A*/T234	−2.57 ± 0.08	−4.2 ± 0.1	1.7 ± 0.1	destabilizing
K230:Tyr	K233, *T234A*	*K230A*/K233/*T234A*	−4.4 ± 0.2	−3.1 ± 0.2	−0.9 ± 0.2	stabilizing
K230:Tyr	*K233A*, *T234A*	*K230A*/*K233A*/*T234A*	−5.3 ± 0.1	−5.6 ± 0.4	0.3 ± 0.4	negligible
K233:Tyr	K230, T234	K230/*K233A*/T234	−3.17 ± 0.05	−3.4 ± 0.1	0.2 ± 0.1	negligible
K233:Tyr	*K230A*, T234	*K230A*/*K233A*/T234	−3.15 ± 0.04	−4.5 ± 0.1	1.3 ± 0.1	destabilizing
K233:Tyr	K230, *T234A*	K230/*K233A*/*T234A*	−4.0 ± 0.2	−4.3 ± 0.3	0.3 ± 0.4	negligible
K233:Tyr	*K230A*, *T234A*	*K230A*/*K233A*/*T234A*	−3.44 ± 0.06	−4.9 ± 0.1	1.5 ± 0.1	destabilizing
T234:Tyr	K230, K233	K230/K233/*T234A*	−3.17 ± 0.05	−4.7 ± 0.2	1.5 ± 0.2	destabilizing
T234:Tyr	*K230A*, K233	*K230A*/K233/*T234A*	−3.15 ± 0.04	−3.3 ± 0.1	0.1 ± 0.1	negligible
T234:Tyr	K230, *K233A*	K230/*K233A*/*T234A*	−2.57 ± 0.08	−4.0 ± 0.3	1.4 ± 0.3	destabilizing
T234:Tyr	*K230A*, *K233A*	*K230A*/*K233A*/*T234A*	−5.18 ± 0.04	−5.4 ± 0.2	0.2 ± 0.2	negligible

Table A6: Free Energies of Ternary Coupling between Mobile Loop Mutants and the Tyrosine Substrate for the Binding of ATP

coupling analyzed	unchanged amino acid	reference protein (0.5 μM Tyr)	$G_{2(expt)}$ (kcal/mol)	$G_{2(add)}$ (kcal/mol)	Δ^3G_{int} (kcal/mol)	effect of coupling on the binding of ATP[a]
(K230:K233):Tyr	(T234)	*K230A*/*K233A*/T234	−3.17 ± 0.05	−2.1 ± 0.2	−1.1 ± 0.2	stabilizing
(K230:K233):Tyr	(*T234A*)	*K230A*/*K233A*/*T234A*	−4.1 ± 0.2	−2.9 ± 0.2	−1.2 ± 0.2	stabilizing
(K230:T234):Tyr	(K233)	*K230A*/K233/*T234A*	−3.17 ± 0.05	−4.6 ± 0.2	1.4 ± 0.2	destabilizing
(K230:T234):Tyr	(*K233A*)	*K230A*/*K233A*/*T234A*	−2.57 ± 0.08	−3.9 ± 0.4	1.3 ± 0.4	destabilizing
(K233:T234):Tyr	(K230)	K230/*K233A*/*T234A*	−3.17 ± 0.04	−3.2 ± 0.5	0.0 ± 0.5	negligible
(K233:T234):Tyr	(*K230A*)	*K230A*/*K233A*/*T234A*	−3.15 ± 0.04	−3.0 ± 0.1	0.2 ± 0.1	negligible

[a] The effect of coupling on the binding of ATP is measured for species 1 relative to the reference species.

pairwise coupling energy, and Δ^3G_{int} is the ternary coupling energy.

REFERENCES

Bhat, T. N., Blow, D. M., Brick, P., & Nyborg, J. (1982) *J. Mol. Biol. 158*, 699−709.

Blanquet, S., Fayat, G., & Waller, J. P. (1975a) *J. Mol. Biol. 94*, 1−15.

Blanquet, S., Fayat, G., Poiret, M., & Waller, J. P. (1975b) *Eur. J. Biochem. 51*, 567−571.

Brick, P., & Blow, D. M. (1987) *J. Mol. Biol. 194*, 287−297.

Brick, P., Bhat, T. N., & Blow, D. M. (1989) *J. Mol. Biol. 208*, 83−98.

Brunie, S., Zelwer, C., & Risler, J. L. (1990) *J. Mol. Biol. 216*, 411−424.

Calendar, R., & Berg, P. (1966) *Biochemistry 5*, 1681−1690.

Carter, P., & Wells, J. A. (1988) *Nature 332*, 564−568.

Carter, P., & Wells, J. A. (1990) *Proteins: Struct., Funct., Genet. 7*, 335−342.

Carter, P. J., Winter, G., Wilkinson, A. J., & Fersht, A. R. (1984) *Cell 38*, 835−840.

Cusack, S., Berthet-Colominas, C., Härtlein, M., Nassar, N., & Leberman, R. (1990) *Nature 347*, 249−255.

Eriani, G., Delarue, M., Poch, O., Gangloff, G., & Moras, D. (1990) *Nature 347*, 203−206.

Fayat, G., Fromant, M., & Blanquet, S. (1977) *Biochemistry 16*, 2570−2579.

Fersht, A. R. (1975) *Biochemistry 14*, 5−12.

Fersht, A. R. (1987) *Biochemistry 26*, 8031−8037.

Fersht, A. R., Knill-Jones, J. W., Bedouelle, H., & Winter, G. (1988) *Biochemistry 27*, 1581−1587.

Fersht, A. R., Matouschek, A., & Serrano, L. (1992) *J. Mol. Biol. 224*, 771−782.

First, E. A., & Fersht, A. R. (1993a) *Biochemistry 32*, 13644−13650.

First, E. A., & Fersht, A. R. (1993b) *Biochemistry 32*, 13651−13657.
First, E. A., & Fersht, A. R. (1993c) *Biochemistry 32*, 13658−13663.
Garcia, G. A., Leatherbarrow, R. J., Eckstein, F., & Fersht, A. R. (1990) *Biochemistry 29*, 1643−1648.
Gibson, T. A. (1984) Ph.D. Thesis, University of Cambridge, U.K.
Hanahan, D. (1985) in *DNA Cloning: A Practical Approach* (Glover, D. M., Ed.) Vol. 1, p 109, IRL Press, Oxford.
Horovitz, A. (1987) *J. Mol. Biol. 196*, 733−735.
Horovitz, A., & Fersht, A. R. (1990) *J. Mol. Biol. 214*, 613−617.
Horovitz, A., & Fersht, A. R. (1992) *J. Mol. Biol. 224*, 733−740.
Hountondji, C., Dessen, P., & Blanquet, S. (1986) *Biochimie 68*, 1071−1078.
Hyafil, F., Jacques, V., Fayat, G., Fromant, M., Dessen, P., & Blanquet, S. (1976) *Biochemistry 26*, 5433−5439.
Kunkel, T. (1985) *Proc. Natl. Acad. Sci. U.S.A. 82*, 488−492.
Leatherbarrow, R. J., & Fersht, A. R. (1987) *Biochemistry 26*, 8524−8528.
Leatherbarrow, R. J., Fersht, A. R., & Winter, G. (1985) *Proc. Natl. Acad. Sci. U.S.A. 82*, 7840−7844.
Mechulam, Y., Dardel, F., Le Corre, D., Blanquet, S., & Fayat, G. (1991) *J. Mol. Biol. 217*, 465−475.
Moras, D. (1992) *Trends Biochem. Sci. 17*, 159−164.
Perona, J. J., Rould, M. A., & Steitz, T. A. (1993) *Biochemistry 32*, 8758−8771.
Rossman, M. G., Moras, D., & Olsen, K. W. (1974) *Nature 250*, 194−199.
Rould, M. A., Perona, J. J., & Steitz, T. A. (1991) *Nature 352*, 213−218.
Steyaert, J., & Wyns, L. (1993) *J. Mol. Biol. 229*, 770−781.
Walker, J. E., Saraste, M., Runswick, M. J., & Gay, N. J. (1982) *EMBO J. 1*, 945−951.
Walker, J. E., Saraste, M., & Gay, N. J. (1984) *Biochim. Biophys. Acta 768*, 164−200.
Webster, T. A., Tsai, H., Kula, M., Mackie, G., & Schimmel, P. (1984) *Science 226*, 1315−1317.
Wells, J. A (1990) *Biochemistry 29*, 8509−8517.
Wells, T. N. C., & Fersht, A. R. (1986) *Biochemistry 25*, 1881−1886.
Wells, T. N. C., Knill-Jones, J. W., Gray, T. E., & Fersht, A. R. (1991) *Biochemistry 30*, 5151−5156.

BI942528K